CHRDL2 promotes cell proliferation by activating the YAP/TAZ signaling pathway in gastric cancer

Lingquan Wang
Ruijin Hospital, Shanghai Jiao Tong University School of Medicine
Wei Xu
Ruijin Hospital, Shanghai Jiao Tong University School of Medicine
Yu Mei
Ruijin Hospital, Shanghai Jiao Tong University School of Medicine
Xufeng Wang
Ruijin Hospital, Shanghai Jiao Tong University School of Medicine
Wentao Liu
Ruijin Hospital, Shanghai Jiao Tong University School of Medicine
Chao Yan
Ruijin Hospital, Shanghai Jiao Tong University School of Medicine
Chen Li
Ruijin Hospital, Shanghai Jiao Tong University School of Medicine
Zhenggang Zhu
Ruijin Hospital, Shanghai Jiao Tong University School of Medicine
Zhentian Ni (nzt12087@rjh.com.cn)
Ruijin Hospital, Shanghai Jiao Tong University School of Medicine

Research Article

Keywords: Gastric cancer, Chordin-like 2, Hippo-YAP, cell proliferation

Posted Date: April 20th, 2022

DOI: https://doi.org/10.21203/rs.3.rs-1561013/v1

Abstract

The encoding product of Chordin-like 2 (CHRDL2) is a member of the chordin family of proteins, which has been shown to be aberrantly expressed in several types of solid tumors. The regulatory underlying mechanisms of CHRDL2, however, remain poorly understood in gastric cancer (GC). In the present study, we determined that CHRDL2 was abnormally upregulated in human gastric cancer tissues compared with adjacent normal tissues. We also showed that CHRDL2 was positively associated with T stage, the pathological stage, distant metastasis, and poor patient prognosis. Moreover, we verified that overexpressing CHRDL2 promoted the proliferation and cell cycle transition of GC cells both *in vitro* and *in vivo*, whereas the opposite results were observed in CHRDL2-depleted cells. In addition, the expression levels of Yes-associated protein (YAP) and transcriptional coactivator with PDZ-binding motif (TAZ) were increased, and the levels of MST2 were decreased in CHRDL2 overexpressing cells. Consistent with previous findings, we observed the converse results in CHRDL2-silenced GC cells. Additionally, knockdown of YAP and overexpression of STK3 (MST2) could reverse the effects of CHRDL2 overexpression-induced proliferation of GC cells *in vitro*. Taken together, CHRDL2 plays a key role by activating the Hippo/YAP pathway in gastric cancer. Therefore, CHRDL2 could serve as a potential therapeutic tool for the treatment of gastric cancer.

1. Introduction

Gastric cancer (GC) is one of the most prevalent digestive malignant tumors, and it is correlated with lower relapse-free survival rates and higher mortality rates compared with other cancers[1,2]. In recent decades, prominent improvements have been realized for many therapeutic strategies, although the overall survival rates have not always been improved, especially in advanced cases[3]. Therefore, it is important to characterize the pathogenesis of cancer to identify effective targets for GC therapy.

Chordin-like 2 (CHRDL2) is a bone morphogenetic protein(BMP)antagonist, and its main function is to prevent BMPs from interacting with their homologous cell surface receptors[4,5]. Previous studies have shown that the levels of *CHRDL2* mRNA were significantly high in breast cancer[6], which was correlated with poor prognosis. It also has been reported that high levels of *CHRDL2* correlate with poor prognosis in colorectal cancer patients[7]. As shown in previous studies[8], CHRDL2 functions as an oncogene in osteosarcoma, promoting proliferation and metastasis by activating the BMP–9/PI3K/AKT pathway. Otherwise, the underlying role of CHRDL2 in the progression of gastric cancer remains unclear.

The Hippo pathway was first discovered in *Drosophila*, where it is considered to be a growth regulatory pathway[9] and also has been shown to be related to organ-size control in animals[10]. Yes-associated protein (YAP) activation results in proliferation and loss of programmed cell death at the organ level[11], whereas the Hippo kinase cascade consists of MST1/2, LATS1/2, and their adaptor proteins in vertebrates[12]. YAP not only serves as a transcriptional coactivator to affect cell growth and apoptosis in several human malignant tumors, but it also acts as a vital effector of the Hippo signaling pathway. In

addition, high levels of YAP are related to the progression of atherosclerosis[13], pancreatitis[14], and liver cancer[15]. Genetic deletion of MST1/2 leads to increased nuclear enrichment of YAP and transcriptional coactivator with PDZ-binding motif (TAZ) and their increased activity as transcriptional coactivators[16] in hepatocellular carcinoma. Conversely, overexpression of MST1/2 results in increased levels of cytoplasmic localization and the degradation of YAP and TAZ[17].

In this work, we found that *CHRDL2* mRNA was clearly upregulated in tumor tissues with gastric cancer using data from the TCGA database, and its high levels were related to poor prognosis in GC patients. Next, we demonstrated that CHRDL2 silencing and overexpression influenced GC cell proliferation and the cell cycle *in vitro*, and affected tumor growth *in vivo*. RNA sequencing analysis revealed that CHRDL2 overexpression was positively correlated to the YAP/TAZ signaling pathway and CHRDL2 played a key role in the MST2/YAP/TAZ signaling pathway in GC cells. We also demonstrated that the mechanism of CHRDL2 was to promote GC cell functional changes and identified it as a potential diagnostic factor and therapeutic target for GC.

2. Results

2.1 CHRDL2 is significantly upregulated in GC cells and tissues and positively correlated with later cancer stage and poor prognosis

As Fig. 1a shows, compared with adjacent nontumor tissues, *CHRDL2* overexpression was positively correlated in tumor tissues by tissue microarrays (TMAs). We estimated the correlation between the level of *CHRDL2* expression in tumor tissues and the clinicopathological parameters of patients with GC. We found that *CHRDL2* expression was positively correlated with tumor size ($P = 0.001$), T stage ($P < 0.001$), TNM stage ($P < 0.001$), and distant metastasis ($P < 0.001$) in tumor tissues, regardless of sex, age, differentiation degree, or Lymph node metastasis (Table 1). Similar to immunohistochemical (IHC) analysis using TMAs, the score of CHRDL2 expression in tumor tissues was significantly higher than in adjacent nontumor tissues (Fig. 1b). Compared with patients who were identified to have low CHRDL2 expression, those with high CHRDL2 levels had shorter overall survival times by Kaplan-Meier analysis (Fig. 1c). In addition, the results were validated using data via searching Gastric adenocarcinoma in The Cancer Genome Atlas (TCGA) database, indicating that *CHRDL2* mRNA expression in tumor tissues was remarkably upregulated (Fig. 1d) and was closely correlated with a later TNM stage (Fig. 1e) and a worse prognosis in those who with high *CHRDL2* expression (Fig. 1f). Furthermore, we verified that CHRDL2 expression was upregulated by using 12 pairs of specimens from GC patients from our center (Fig. 1g). Moreover, the expression of CHRDL2 in 6 GC cell lines was significantly higher than in normal gastric epithelial GES-1 cell by Western blotting and Reverse transcription–polymerase chain reaction (RT-PCR) (Fig. 1h).

2.2 CHRDL2 overexpression promotes GC cell proliferation in vitro *and* in vivo

To elucidate the effect of CHRDL2 on cell behavior, CHRDL2 overexpression GC cells were constructed by transfection with a CHRDL2 expression plasmid (MGC-803/CHRDL2-OE and AGS/CHRDL2-OE), (Fig. 2a). As Cell Counting Kit-8 (CCK8), EdU and colony formation assays showed, CHRLD2 overexpression significantly improved the cell proliferation and colony formation capacities of MGC-803 and AGS cells (Fig. 2b–2d). Moreover, flow cytometry assays demonstrated that CHRDL2 play a key role in promoting the cell cycle transition from G0/G1 phase to S phase (Fig. 2e). Using an *in vivo* subcutaneous xenograft model, we further demonstrated that CHRRDL2 overexpression definitely promoted the tumor-forming capacity of MGC-803 cells (Fig. 2f). We also found that the Ki-67 index in subcutaneous tumors formed by MGC-803/CHRDL2-OE cells was higher through immunohistochemical (IHC) staining compared with those generated by MGC-803/NC cells (Fig. 2g).

2.3 GC cell proliferation inhibited by knockdown of CHRDL2 in vitro *and* in vivo

To identify the effect of CHRDL2 on GC cell proliferation, we used lentivirus-mediated knockdown CHRDL2 expression in HGC-27 and MGC-803 cells. To this end, we first used Western blotting and RT-PCR to determine the silencing efficiency (Fig. 3a). As we had hypothesized, cell proliferation, colony formation, and the cell cycle transition effects were all reversed by silencing CHRDL2 (Fig. 3b–3e). Furthermore, knockdown of CHRDL2 also inhibited the growth ability of subcutaneous tumors in nude mice. Compared with control MGC-803 cells, the sh-CHRDL2 group had low ability to form tumors (Fig. 3f). Additionally, IHC staining showed that the Ki-67 index of the subcutaneous tumors that were formed by sh-CHRDL2 MGC-803 cells was lower than that of control cells (Fig. 3g).

2.4 Upregulation of CHRDL2 activates the YAP/TAZ pathway

To further explore how CHRDL2 promotes GC cell proliferation, RNA sequencing was performed with AGS/CHRDL2-OE cells and AGS/Ctrl cells (Fig. 4a). Kyoto Encyclopedia of Genes and Genomes (KEGG) analysis results for signaling pathway enrichments indicated that these differentially expressed genes were markedly related to transcriptional mis-regulation in cancer, the Hippo pathway, and the ErbB signaling pathway (Fig. 4b). Therefore, we chose the top related 30 genes enriched from these pathways, and RT-PCR results (Fig. 4c) showed they had a close connection to the Hippo pathway. We also showed by RT-PCR (Fig. 4d) that the expression levels of *STK3*, *YAP*, and *TAZ* were significantly increased in MGC-803/CHRDL2-OE and AGS/CHRDL2-OE cells, whereas the opposite tendency was detected in MGC-803/sh-CHRDL2 and HGC-27/sh-CHRDL2 cells. Additionally, it was clear that the expression of YAP and TAZ was significantly elevated in MGC-803/CHRDL2-OE and AGS/CHRDL2-OE cells in Q-PCR and Western blots (Fig. 4e, 4g), whereas the opposite trend occurred in MGC-803/sh-CHRDL2 and HGC-27/sh-CHRDL2 cells (Fig. 4f, 4h). We also found that CHRDL2 silencing facilitated the protein and mRNA levels of MST2, and this result was contradicted in CHRDL2 overexpression cells. In summary, these results

highlighted that CHRDL2 may exert cancer-promoting influence on GC cells by activating the YAP/TAZ signaling pathway.

2.5 CHRDL2 promotes GC cells proliferation through the MST2/YAP/TAZ signaling pathway

Mst2 kinases have been reported to be central regulators of the Hippo pathway. When they are activated, resulting in phosphorylating of YAP and TAZ, this leads to their cytoplasmic sequestration and ultimate degradation[18,19]. Our results showed that CHRDL2 overexpression increased the levels of YAP/TAZ and decreased the levels of MST2. Moreover, when CHRDL2 was silenced, this regulation was impaired. To unravel the molecular mechanism by which CHRDL2 modulates YAP/TAZ and MST2 in GC cells, we transfected pcDNA-MST2 or si-YAP into MGC-803/CHRDL2-OE and AGS/CHRDL2-OE cells. We chose one short-interfere RNA (Si-RNA) that presented high interference efficiency for the expression of YAP from three sequences(Fig. 5a) First, STK3 overexpression downregulated CHRDL2-mediated levels of YAP and TAZ proteins and mRNA. YAP silencing in CHRDL2-OE cells led only to the reduction of YAP, whereas the expression of MST2 was not influenced (Fig. 5b–5e). Next, we verified the influence of YAP knockdown and MST2 overexpression on the overexpression of CHRDL2 that resulted in promoting proliferation *in vitro*. We found that YAP knockdown and MST2 overexpression reversed the CHRDL2 overexpression-induced increase in GC cell proliferation by CCK-8 assay and clone formation (Fig. 5f–5i). Moreover, we also found the effect of YAP silencing and STK3 overexpression on CHRDL2-induced cell cycle transition. This confirmed that silencing YAP and STK3 overexpression served to counteract the CHRDL2-induced cell cycle transition of GC cells, as shown by flow cytometry (Fig. 5f, 5g). These results indicated that CHRDL2 exerts its function on the MST2-YAP/TAZ axis.

2.6 CHRDL2 is negatively correlated with MST2 and positively correlated with YAP and TAZ in subcutaneous tumors

To confirm the correlation between CHRDL2, MST2, YAP, and TAZ, we performed IHC analysis to evaluate their levels in subcutaneous xenograft tumors. These experiments indicated that YAP and TAZ were highly expressed while MST2 was downregulated in CHRDL2-overexpressing subcutaneous tumors, and the opposite results were detected in CHRLDL2-silenced subcutaneous tumors (Fig. 6a, 6b). These results further verified that CHRDL2 may act as an oncogene via the YAP/TAZ signaling pathway in GC.

3. Discussion

By analyzing public datasets, we identified that *CHRDL2* was related to later stage and higher mortality in GC patients. Thus, we inferred that *CHRDL2* may serves as a positive factor in GC. CHRDL2 is known as a secreted protein and also is a member of the chordin family of proteins, which contain a cysteine-rich pro-collagen repeat domain and are related to the transforming growth factor beta superfamily. Moreover, we verified that CHRDL2 was upregulated in tumor tissues and was also associated with poor prognosis[6]. Then, we identified that CHRDL2 was significantly overexpressed in GC samples from TMAs, and this

was correlated to later T stage, TNM stage, and distant metastasis. We also determined that upregulated CHRDL2 was significantly correlated with a short overall survival (OS) in GC patients and demonstrated the effect of CHRDL2 on promoting GC *in vivo* and *in vitro*. Moreover, overexpressing CHRDL2 significantly facilitated GC cell proliferation as detected by EdU, CCK-8, and colony formation assays, and also influenced the cell cycle as shown by flow cytometry. In contrast, the knockdown of CHRDL2 had the converse effects *in vitro*. Additionally, xenograft tumor assays provided evidence suggesting that CHRDL2 had a positive effect on GC growth *in vivo*. Therefore, CHRDL2 was identified as a cancer-promoting gene contributing to the growth of GC cells.

Mechanistically, RNA sequencing analysis with KEGG pathway enrichment that was verified by Western blotting indicated that the Hippo pathway was correlated with CHRDL2. The Hippo pathway has been shown to be an evolutionarily conserved signaling pathway that also serves as vital role in diverse biological functions including development, homeostasis, and the regeneration of tissues and organs[22–24]. Moreover, YAP is the key downstream effector of this pathway, which results in the core kinase cascade in this signaling pathway[25]. Additionally, YAP has been shown to be connected with many forms of cancer[26,27] and its paralog, TAZ, which is known as the WW-domain containing transcription regulator-1 (WWTR1), is also a key component of the Hippo pathway[28]. The Hippo pathway influences cell function, in terms of cell proliferation and apoptosis, by inhibiting the YAP and TAZ transcriptional co-activators. This pathway also leads to stemness in response to a series of extracellular and intracellular signals[10,29]. In the present study, we demonstrated that MST2, which is a kinase of the Sterile 20-like (STE20) superfamily, is also related to cell proliferation. Its primary function is antiproliferative and it promotes apoptosis by regulation of downstream effectors[30].

However, no evidence has been identified connecting the YAP signaling pathway and CHRDL2 in previous research. Therefore, we verified that CHRDL2 was positively associated with the YAP signaling pathway and that CHRDL2 silencing could reverse the function of this pathway. Additionally, knockdown of YAP recovered the cell proliferation and cell cycle characteristics of GC cells. Moreover, our data showed the negative correlations between CHRDL2 and MST2, and the overexpression of MST2 also could reverse the growth and cell cycle behavior of GC cells, which was caused by CHRDL2 overexpression. Consequently, CHRDL2 promoted growth and proliferation via the YAP signaling pathway.

In conclusion, our results demonstrated the mechanisms of CHRDL2 in GC cells as illustrated in the model shown in Fig. 6b. This figure depicts the foundation for future monitoring indicators of GC and the possibility of therapeutic target selection. Our study had some shortcomings and needs further molecular mechanism research to be conducted to further elucidate the role of CHRDL2 in GC.

4. Materials And Methods

4.1 TMA and tissue samples

In this study, we used TMs containing 80 tumor tissues and 80 adjacent normal tissues obtained from GC patients (HStmA180Su13; Shanghai Outdo Biotech, Shanghai, China). An anti-CHRDL2 antibody was used to stain them, the staining intensity was scored and the CHRDL2 staining score was calculated. All 12 pairs of tumor and normal tissues were obtained from Ruijin Hospital, Shanghai Jiao Tong University School of Medicine. All patients mentioned in this study had not received therapy, and the clinical stage for each section was obtained according to the TNM stage of American Joint Committee on Cancer and International Union Against Cancer(AJCC/UICC) for GC, 8th edition[20,21].

4.2 Cell culture and experiments

Gastric-adenocarcinoma cell lines HGC-27, MGC-803, SGC-7901, HS-746T, BGC-823, and MKN-45, and the human immortalized gastric cell line GES-1 were obtained from the Cell Bank of the Chinese Academy of Sciences. We cultivated cells in Dulbecco's Modified Eagle Medium or RPMI-1640 medium containing 10% fetal bovine serum (Gibco Waltham, MA, USA) and 1% penicillin-streptomycin in a humidified incubator with 5% CO_2 at 37°C.

STK3 cDNA was synthesized and inserted into pCDNA3.1 plasmid (PPL; Nanjing, Jiangsu, China), while using an empty pcDNA3.1 plasmid as a control. To silence the expression of YAP, we generated siRNA-YAP and use siRNA-NC as a control by Genomeditech (Shanghai, China). The full-length CHRDL2 cDNA was inserted into a lentiviral GFP-Puro vector (PPL; Nanjing), and we also cloned a small hairpin RNA (shRNA) targeting *CHRDL2* into the piLenti-shRNA-GFP-Puro vector by PPL (Nanjing). For transfection, we first transduced MGC-803, HGC-27, and AGS cells with the lentiviruses mentioned earlier for 24 h, and then we replaced the medium with 5 μg/mL puromycin (Beyotime Biotechnology, Beijing, China) after 48 h. Using Lipofectamine 3000 (Invitrogen, Carlsbad, CA, USA) to complete the transfection, we then collected the cells after 48 h of transfection.

4.3 RNA extraction and real-time quantitative polymerase chain reaction

First, we used TRIzol reagent (Vazyme, Nanjing, China) to extract the total RNA following the manufacturer's protocol. Then, RNA samples were reverse transcribed into cDNA using a Reverse Transcription System (Toyobo, Osaka, Japan). Messenger RNA (mRNA) levels were determined using ChamQ Universal SYBR qPCR Master Mix (Vazyme) on an Applied Biosystems 7900HT sequence detection system (Applied Biosystems, Foster City, CA USA). Using the $2 - \Delta\Delta Ct$ method, the relative expression of mRNA levels was determined relative to *GAPDH*. All the primers used are presented in Supplementary Table S1.

4.4 Western blotting analysis

Using a standard protocol, the total protein extraction of GC cells was performed in RIPA lysis buffer (Solarbio, Beijing, China) supplemented with phenylmethylsulfonyl fluoride (PMSF; Solarbio) and a protease inhibitor cocktail (Roche, Basel, Switzerland). We then determined the concentration of protein by BCA assay (Pierce, Thermo Fisher, Waltham, MA, USA). Western blotting was performed following a

previously published protocol. The candidate antigens were detected by antibodies (all antibodies are described in detail in Supplementary Table S2). All bands were captured using a Tanon imaging system.

4.5 Cell proliferation assays

We determined the rates of cell proliferation using an EdU Labeling Kit (Beyotime Biotechnology, Haimen, China) and a Cell Counting Kit-8 (CCK-8; Dojindo, Shanghai, China). All experimental procedure followed the manufacturers' instructions. To conduct the colony formation assay, we put 1×10^3 GC cells/per well into six-well plates for cultivation for 14 days.

4.6 IHC staining

For subcutaneous tumors, we made formalin-fixed and paraffin-embedded specimens, and then cut these into 5 μm thick sections and fixed them on glass slides. These sections were then incubated with different antibodies. To determine the ratio of positive tumor cells, we performed semiquantitative evaluation by assessing the percentage of positive cells. The details are as follow: 0 = 5–25%, 1 = 26–50%, 2 = 51–75%, and 3 = ≥ 75%. We also evaluated the expression levels of CHRDL2, MST2, TAZ, Ki-67, and YAP by scoring the intensity of stained cancer cells as follows: 0 (no staining), 1 (weak staining, light yellow), 2 (moderate staining, yellow), and 3 (strong staining, brown). Above all, scores ≥ 3 were regarded as high expression, and those < 3 were considered low expression.

4.7 Cell cycle analysis

We collected 5×10^5 cells in six-well plates, fixed with 75% ethanol, which were placed at 4°C overnight. Then, we resuspended the cells in 400 μL of PI/RNase Staining Buffer (Biosciences, NC, USA), and stained these cells for 30 min at room temperature in a dark room. Finally, we analyzed the cell cycle using flow cytometry.

4.8 Animal tumor transplantation

All animal experiments were approved by the local Laboratory Animal Ethics Committee of Ruijin Hospital (Shanghai, China). We purchased three- to four-week-old male BALB/c-nude mice from the Chinese Academy of Sciences (Shanghai, China) and divided them into two groups (n = 5 per group). Mice were subcutaneously injected with 5×10^6 MGC-803/CHRDL2 or MGC-803/vector cells. For measurements, we determined the tumor (a) length and (b) width every four days. The method of calculating tumor volumes was as follows: volume = 1/2 (a × b2). After 32 days, we killed the mice and harvested the tumors, which we stored at -80°C for further research.

4.9 Statistical analysis

We performed statistical analysis using SPSS 21.0 and GraphPad Prism 7.0. All data are shown as the mean ± SD from three or more independent experiments. Independent-sample *t* tests were performed between cell proliferation assay samples, qPCR samples, and for tumor weight and sizes between two groups. We estimated the correlation of CHRDL2 expression with the clinicopathological characteristics of GC using the Chi-square (χ2) test. Spearman's correlation analysis was conducted to assess the

association between CHRDL2, MST2, and YAP/TAZ in paraffin-embedded clinical tumor tissues. A P value < 0.05 was regarded as statistically significant (**p < 0.05; ***p < 0.01; ****p < 0.001).

Abbreviations

CHRDL2: Chordin-like 2; GC: gastric cancer; BMP: bone morphogenetic protein; GES-1: immortalized gastric epithelial cell line; IHC: immunohistochemistry; YAP: Yes-associated protein; TAZ: WW domain containing transcription regulator 1, or WWTR1; MST2: mammalian sterile 20-like kinase 2; CCK-8: Cell Counting Kit-8; RNA-seq: RNA sequencing; KEGG: Kyoto Encyclopedia of Genes and Genomes; qRT-PCR: Quantitative real-time PCR; SD: Standard deviation; OS: Overall survival

Declarations

Authors' contribution

ZTN, ZGZ, and LQW contributed to conceptualization; WX, CY, and XFW contributed to formal analysis; MY and JFL contributed to investigation; YM, CL, and WX contributed to methodology and resources; LQW and YM contributed to writing—original draft; LQW, ZTN and ZGZ contributed to review and editing. All authors read and approved the final manuscript.

Acknowledgments

Not applicable.

Availability of data and materials

The datasets used and analyzed during the current study are available within the manuscript and its figures and tables.

Ethical approval and consent to participate and publication

This research was approved by the Ruijin Hospital Ethics Committee of Shanghai Jiao Tong University of Medicine and written informed consent was obtained from all patients before enrolling in the research program. All patients involved in our study provided written consent for publication.

Funding

This work was supported by Shanghai Jiao Tong University School of Medicine, Project Number: TMSZ-2020-205. This work was also supported by the National Natural Science Foundation of China, Project Number: 81871904.

Conflict of Interest

All authors declare no competing interests.

References

1. Bray F, Ferlay J, Soerjomataram I, Siegel RL, Torre LA, Jemal A. Global cancer statistics 2018: GLOBOCAN estimates of incidence and mortality worldwide for 36 cancers in 185 countries. CA Cancer J Clin 2018;**68**(6):394–424.
2. Collaborators GBDSC. The global, regional, and national burden of stomach cancer in 195 countries, 1990–2017: a systematic analysis for the Global Burden of Disease study 2017. Lancet Gastroenterol Hepatol 2020;**5**(1):42–54.
3. Luo G, Zhang Y, Guo P, Wang L, Huang Y, Li K. Global patterns and trends in stomach cancer incidence: Age, period and birth cohort analysis. Int J Cancer 2017;**141**(7):1333–44.
4. Fujisawa T, Huang Y, Sebald W, Zhang JL. The binding of von Willebrand factor type C domains of Chordin family proteins to BMP-2 and Tsg is mediated by their SD1 subdomain. Biochem Biophys Res Commun 2009;**385**(2):215–9.
5. Nakayama N, Han CY, Cam L, Lee JI, Pretorius J, Fisher S, *et al.* A novel chordin-like BMP inhibitor, CHL2, expressed preferentially in chondrocytes of developing cartilage and osteoarthritic joint cartilage. Development 2004;**131**(1):229–40.
6. Wu I, Moses MA. BNF-1, a novel gene encoding a putative extracellular matrix protein, is overexpressed in tumor tissues. Gene 2003;**311**:105–10.
7. Sun J, Liu X, Gao H, Zhang L, Ji Q, Wang Z, *et al.* Overexpression of colorectal cancer oncogene CHRDL2 predicts a poor prognosis. Oncotarget 2017;**8**(7):11489–506.
8. Chen H, Pan R, Li H, Zhang W, Ren C, Lu Q, *et al.* CHRDL2 promotes osteosarcoma cell proliferation and metastasis through the BMP-9/PI3K/AKT pathway. Cell Biol Int 2021;**45**(3):623–32.
9. Xu T, Wang W, Zhang S, Stewart RA, Yu W. Identifying tumor suppressors in genetic mosaics: the Drosophila lats gene encodes a putative protein kinase. Development 1995;**121**(4):1053–63.
10. Yu FX, Zhao B, Guan KL. Hippo Pathway in Organ Size Control, Tissue Homeostasis, and Cancer. Cell 2015;**163**(4):811–28.
11. Gumbiner BM, Kim NG. The Hippo-YAP signaling pathway and contact inhibition of growth. J Cell Sci 2014;**127**(Pt 4):709–17.
12. Sebio A, Lenz HJ. Molecular Pathways: Hippo Signaling, a Critical Tumor Suppressor. Clin Cancer Res 2015;**21**(22):5002–7.
13. Wang L, Luo JY, Li B, Tian XY, Chen LJ, Huang Y, *et al.* Integrin-YAP/TAZ-JNK cascade mediates atheroprotective effect of unidirectional shear flow. Nature 2016;**540**(7634):579–82.
14. Morvaridi S, Dhall D, Greene MI, Pandol SJ, Wang Q. Role of YAP and TAZ in pancreatic ductal adenocarcinoma and in stellate cells associated with cancer and chronic pancreatitis. Sci Rep 2015;**5**:16759.
15. Machado MV, Michelotti GA, Pereira TA, Xie G, Premont R, Cortez-Pinto H, *et al.* Accumulation of duct cells with activated YAP parallels fibrosis progression in non-alcoholic fatty liver disease. J Hepatol 2015;**63**(4):962–70.

16. Zhou D, Conrad C, Xia F, Park JS, Payer B, Yin Y, *et al.* Mst1 and Mst2 maintain hepatocyte quiescence and suppress hepatocellular carcinoma development through inactivation of the Yap1 oncogene. Cancer Cell 2009;**16**(5):425–38.
17. Loforese G, Malinka T, Keogh A, Baier F, Simillion C, Montani M, *et al.* Impaired liver regeneration in aged mice can be rescued by silencing Hippo core kinases MST1 and MST2. EMBO Mol Med 2017;**9**(1):46–60.
18. Song H, Mak KK, Topol L, Yun K, Hu J, Garrett L, *et al.* Mammalian Mst1 and Mst2 kinases play essential roles in organ size control and tumor suppression. Proc Natl Acad Sci U S A 2010;**107**(4):1431–6.
19. Wu H, Wei L, Fan F, Ji S, Zhang S, Geng J, *et al.* Integration of Hippo signalling and the unfolded protein response to restrain liver overgrowth and tumorigenesis. Nat Commun 2015;**6**:6239.
20. Brierley JD, Gospodarwicz MK, Wittekind C, Amin MB. TNM classifcation of maligant tumours. 8th ed. *Oxford: Wiley Black well* 2017.
21. Amin MB, Edge SB, Greene FL, Brierley JD. AJCC cancer staging manual. 8th ed. *New York*: *Springer* 2017.
22. Moya IM, Halder G. Hippo-YAP/TAZ signalling in organ regeneration and regenerative medicine. Nat Rev Mol Cell Biol 2019;**20**(4):211–26.
23. Misra JR, Irvine KD. The Hippo Signaling Network and Its Biological Functions. Annu Rev Genet 2018;**52**:65–87.
24. Maugeri-Sacca M, De Maria R. The Hippo pathway in normal development and cancer. Pharmacol Ther 2018;**186**:60–72.
25. Huang J, Wu S, Barrera J, Matthews K, Pan D. The Hippo signaling pathway coordinately regulates cell proliferation and apoptosis by inactivating Yorkie, the Drosophila Homolog of YAP. *Cell* 2005;**122**(3):421 – 34.
26. Mao W, Mai J, Peng H, Wan J, Sun T. YAP in pancreatic cancer: oncogenic role and therapeutic strategy. Theranostics 2021;**11**(4):1753–62.
27. Maehama T, Nishio M, Otani J, Mak TW, Suzuki A. The role of Hippo-YAP signaling in squamous cell carcinomas. Cancer Sci 2021;**112**(1):51–60.
28. Piccolo S, Dupont S, Cordenonsi M. The biology of YAP/TAZ: hippo signaling and beyond. Physiol Rev 2014;**94**(4):1287–312.
29. Yang WH, Chi JT. Hippo pathway effectors YAP/TAZ as novel determinants of ferroptosis. Mol Cell Oncol 2020;**7**(1):1699375.
30. Wu S, Huang J, Dong J, Pan D. hippo encodes a Ste-20 family protein kinase that restricts cell proliferation and promotes apoptosis in conjunction with salvador and warts. Cell 2003;**114**(4):445–56.

Tables

Table 1 Correlations between CHRDL2 expression and clinical characteristics in GC patients.

Clinicopathologic parameters	Case(n=80)	CHRDL2 expression		*P*-value
		Low	High	
Total	80	22	58	
Gender				0.703
Male	56	15	41	
Female	24	7	17	
Age				0.944
≥60	55	15	40	
<60	25	7	18	
Tumor (cm)				0.001
≥3.0	49	8	41	
<3.0	31	14	17	
Differentiation				
Well, moderately	38	12	26	0.096
Poorly, undifferentiated	42	10	32	
T stage				0.000
T1+T2	19	15	7	
T3+T4	61	7	51	
Lymph node metastasis				0.086
N0+N1	38	11	27	
N2+N3	42	11	31	
Distant metastasis				0.001
M0	74	22	52	
M1	6	0	6	
Pathological stage				0.000
I+II	32	17	15	
III+IV	48	5	43	

Table 2 Univariate and multivariate analysis of clinic pathological factors for overall survival in GC patients.

Variables	Univariate analysis		Multivariate analysis	
	HR(95% CI)	*P*	HR(95% CI)	*P*
CHRDL2(low vs. high)	3.353（1.212-6.243）	0.001	2.497（1.317-4.735）	0.005
Age(≥60 vs. <60)	0.893(0.424-1.914)	0.792		
Gender (male vs. female)	0.917（0.399-2.029）	0.881		
Tumor size(≥3 vs. <3)	1.324（0.911-2.341）	0.094		
T stage (T1–2 vs. T3–4)	1.221（1.056-2.734）	0.017	1.109（1.321-2.123）	0.029
Lymph node metastasis (N0-1 vs. N2–3)	2.484（0.621-5.363）	0.619		
Distant metastasis(M0vs. M1)	1.562（1.174-2.079）	0.004	1.372（1.081-1.828）	0.015
Pathological stage (I–II vs. III–IV)	1.779（1.201-2.529）	0.002	1.512（1.119-2.342）	0.031

Figures

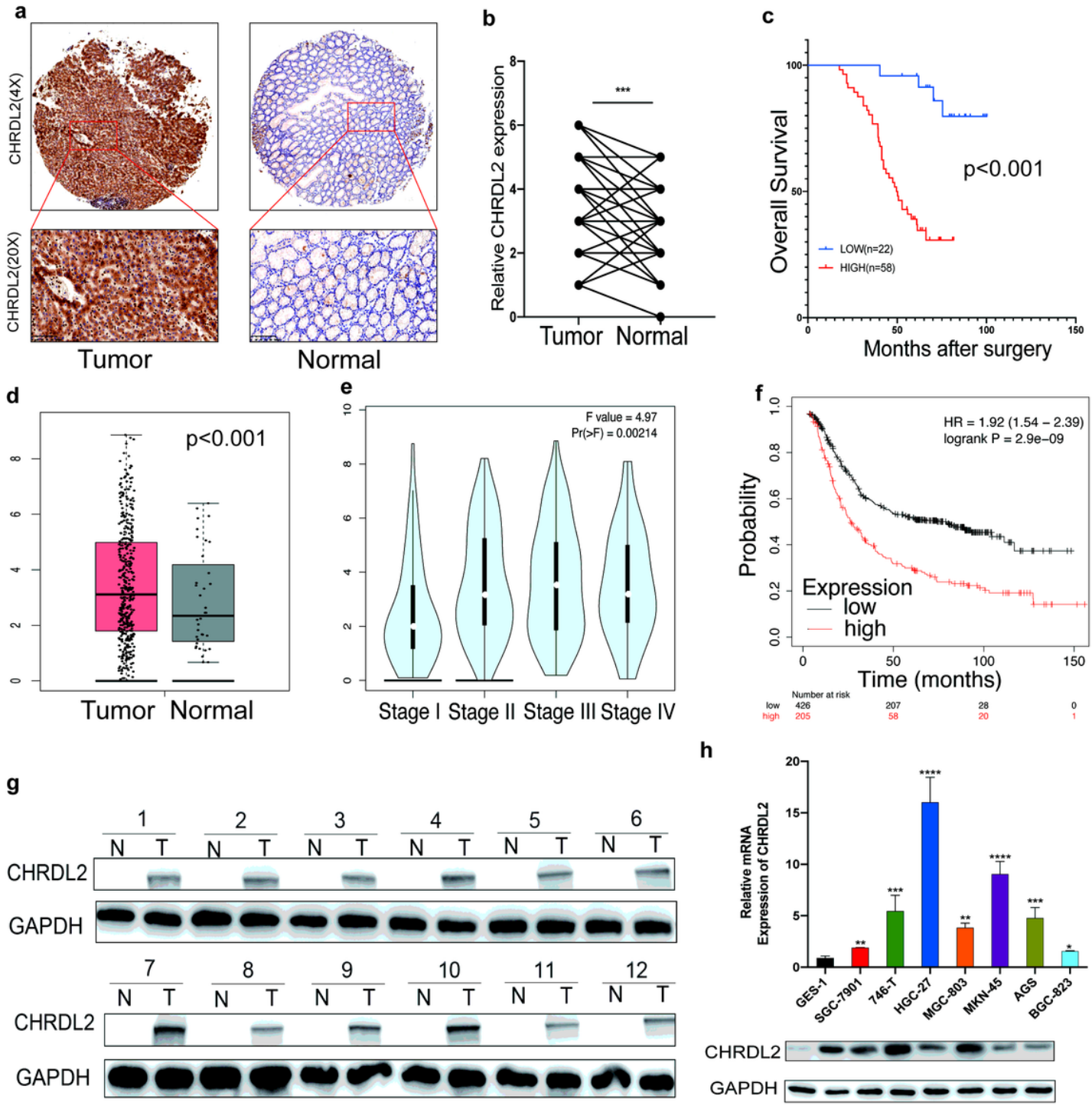

Figure 1

CHRDL2 expression in GC tissues and cells and correlation with the prognosis of GC patients. a Representative IHC staining images in TMA-containing tumor tissues and matched tumor-adjacent tissues with GC. **b** IHC score analysis of two groups conducted by Wilcoxon rank-sum test suggested a discrepancy. **c** K-M curves of CHRDL2 using survival data from TMAs. **d–f** CHRDL2 expression in GC differed based on the sample type, individual cancer stage and prognosis from the TCGA database. **g** Compared with adjacent normal tissues, CHRDL2 was overexpressed in tumor tissues from 12 patients in

our center. **h** The expression level of CHRDL2 differed between six GC cells and GES-1 by Western blotting and RT-PCR. ***P* < 0.05, ****P* <0. 01, ****P* < 0.001. Data are shown as the mean± SD (n ≥ 3).

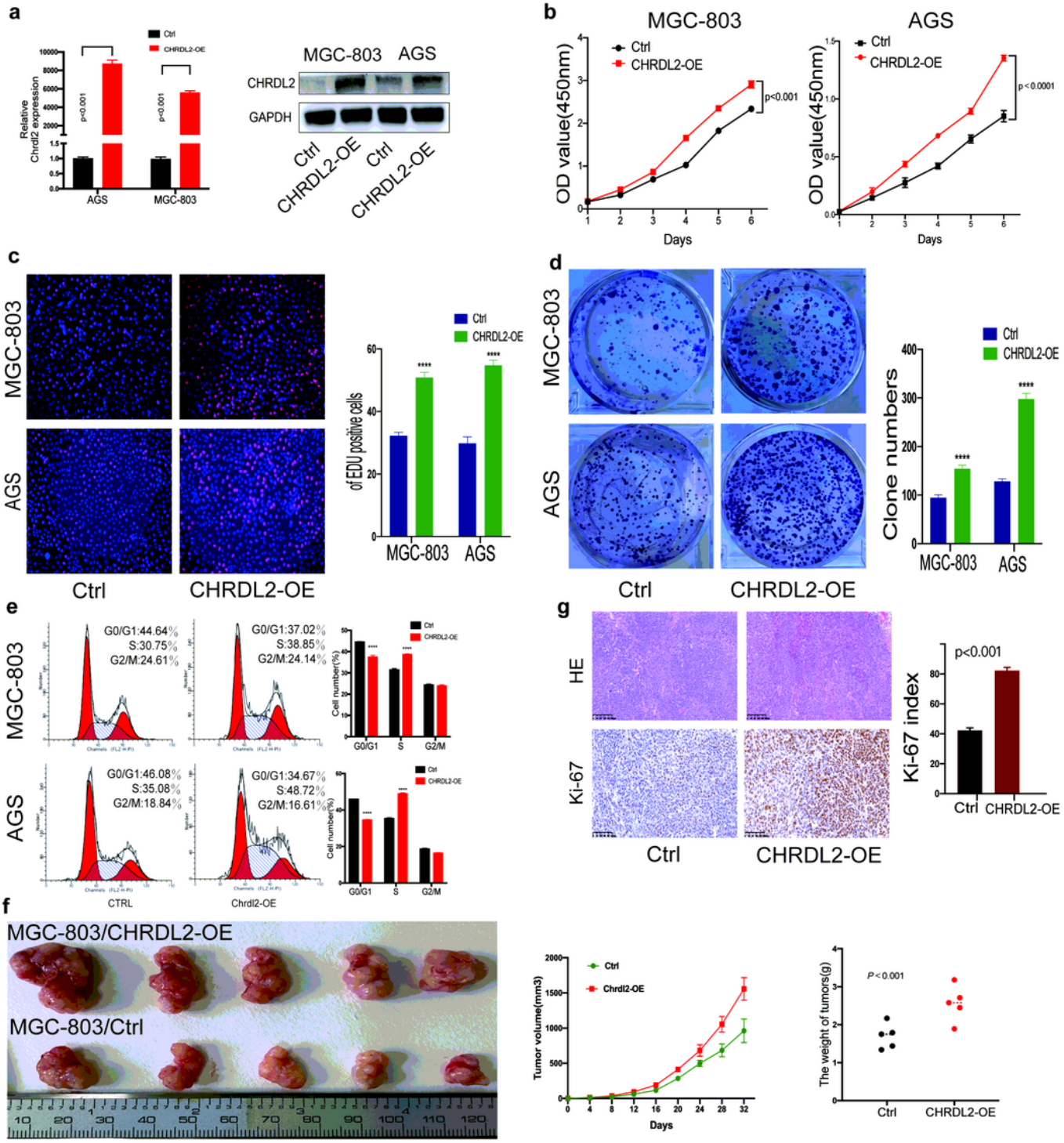

Figure 2

Overexpression of CHRDL2 promotes GC cells proliferation. a Western-blotting and RT-PCR indicate CHRDL2-overexpression in MGC-803 and AGS cells was successful performed. **b–c** CHRDL2 promote cell

proliferation as detected by CCK8 assay and EdU in MGC-803 and AGS cell lines. **d** Colony formation revealed that CHRDL2 increased the abilities of MGC-803 and AGS cells. **e** CHRDL2 induced the cell cycle transition from G0/G1 to S as shown by flow cytometry. **f** Xenograft of subcutaneous tumors formed by MGC-803/CHRDL2-OE cells were bigger than those developed by the control group. The charts also revealed the same tendency for the growth curve of tumor and final tumor weight, respectively. **g** IHC staining analysis, indicating that the index of Ki-67 in the overexpression group was higher than in the control group in xenograft tumors. All results were obtained from at least three independent experiments. $*p < 0.05$; $**p < 0.01$; $***p < 0.001$.

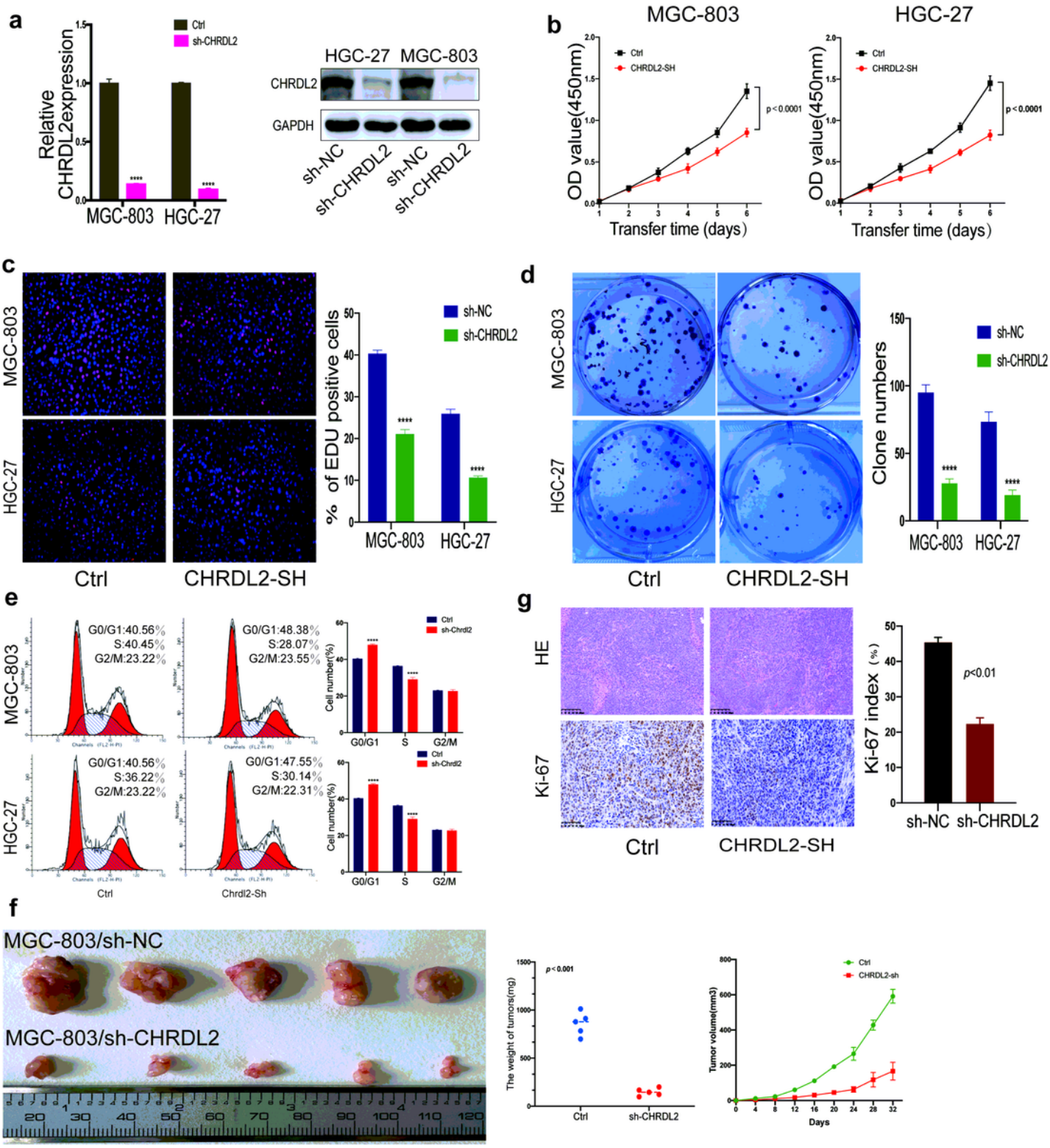

Figure 3

Knockdown of CHRDL2 inhibits cell proliferation both *in vitro* and *in vivo*. **a** Western-blotting and RT-PCR indicating the knockdown efficiency of CHRDL2 in MGC-803 and HGC-27 cells. **b–c** As CCK8 assay and EdU reveal, silencing CHRDL2 decreased the growth ability in MGC-802 and HGC-27 cell lines. **d** Colony formation assay showing that knockdown of CHRDL2 significantly inhibited the growth of MGC-803 and HGC-27 cell lines. **e** Silencing CHRDL2 resulted in cell cycle hindering in G0/G1. **f** The subcutaneous

tumors formed by MGC-803/sh-CHRDL2 cells were more significantly developed than MGC-803/ctrl cells. The charts also revealed the same tendency for the curve of tumor growth curve and tumor weight, respectively. **g** The Ki-67 index was investigated through IHC in xenograft tumors. All data were acquired from three independent experiments. *$p < 0.05$; **$p < 0.01$; ***$p < 0.001$. Results are shown as mean ± SD.

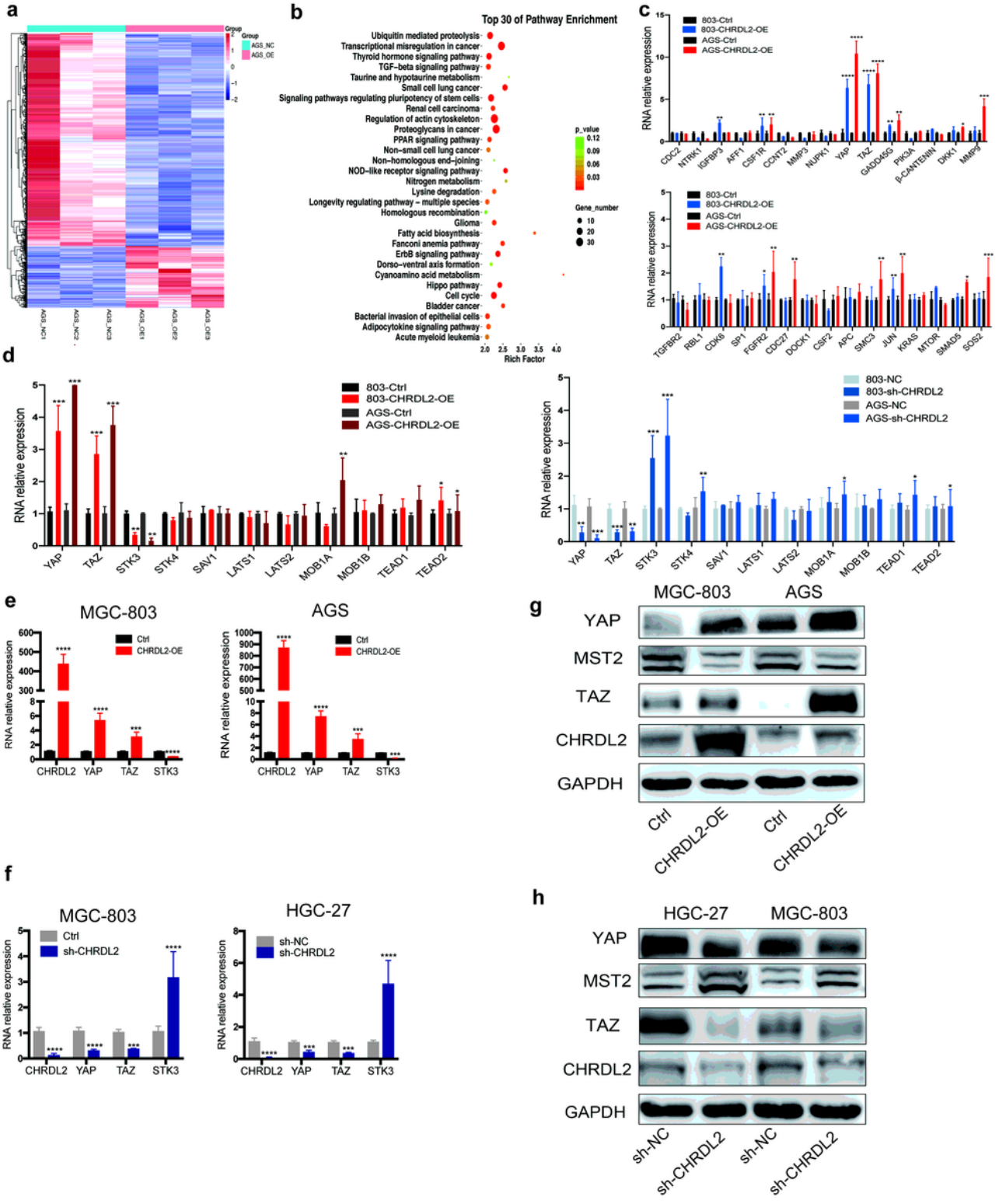

Figure 4

Cancer-promoting effects of CHRDL2 function through the activation of the Hippo/YAP pathway. a Heatmap showing differentially expressed genes obtained from RNA-seq data AGS/CHRDL2-OE versus AGS/NC cells (n = 3). **b** KEGG pathway enrichment analysis of differentially expressed genes in RNA-seq data from AGS/CHRDL2-OE versus AGS/NC cells (n = 3). **c** Real-time PCR showing the top 15 differentially expressed genes selected from RNA-seq in MGC-803/CHRDL2-OE and AGS/CHRDL2-OE cell lines. **d, f** Western blotting analysis of CHRDL2's influence on the YAP/TAZ pathway in MGC-803 and AGS cells. **e, g** Real-time PCR revealing that CHRDL2 resulted in the differential expression of the Hippo/YAP pathway. *$p < 0.05$; **$p < 0.01$; ***$p < 0.001$.

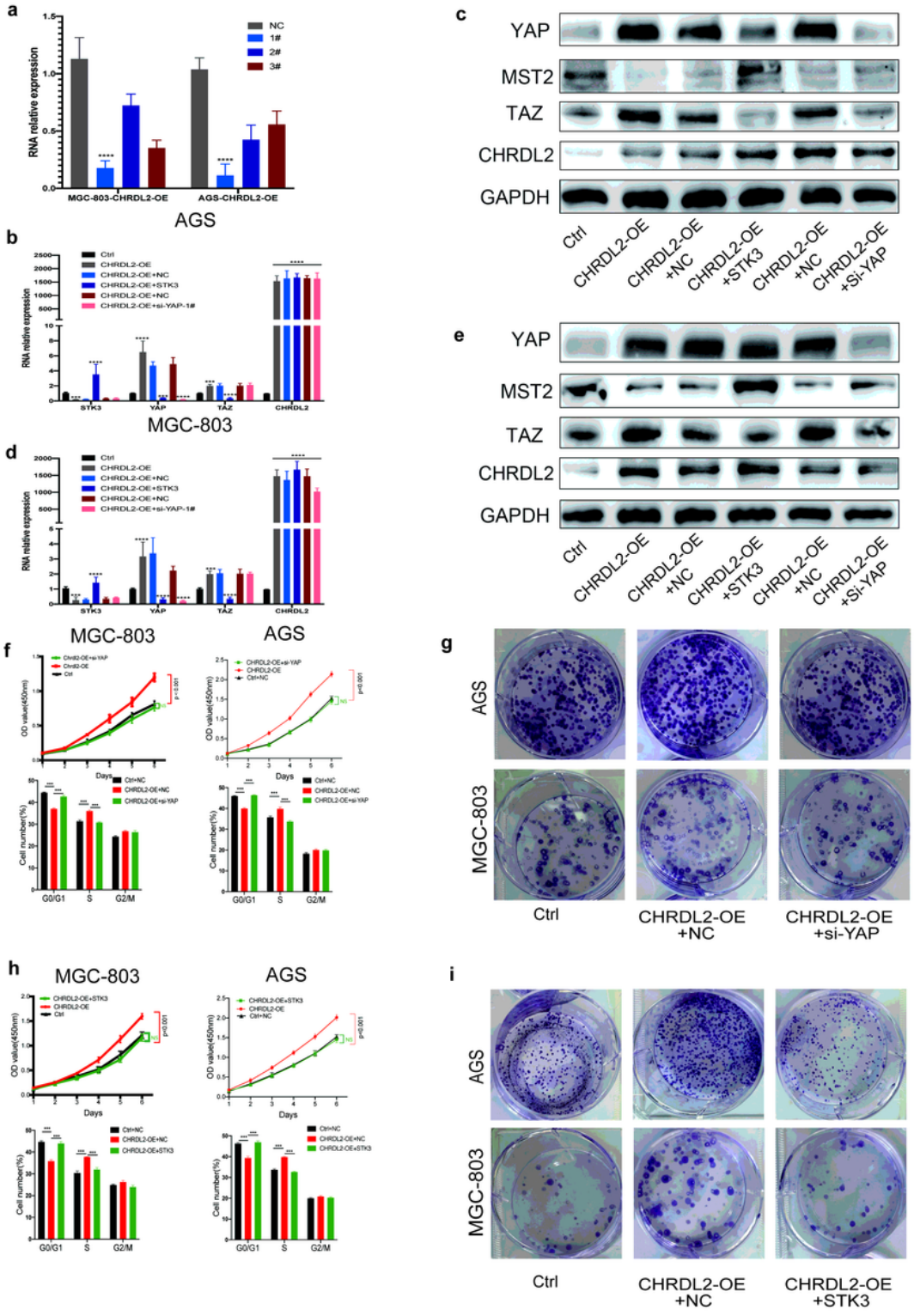

Figure 5

CHRDL2 overexpression induces tumor progression in GC cells and can be reversed by YAP silencing and STK3 overexpression. a RT-PCR shows the interference efficiency of three YAP-targeting siRNA in MGC-803- and AGS-CHRDL2-OE cells. **b, c, d, e** Real-time PCR and Western blotting showing the different expression of YAP, TAZ and MST2 in AGS/CHRDL2-OE and MGC-803/CHRDL2-OE cells co-transfected with pc-DNA-STK3 or si-YAP. **f, g** Silencing YAP can abolished the growth abilities of GC cells acquired by

CHRDL2 overexpression, as demonstrated by CCK-8 assay, flow cytometry and colony formation assay. **h, i** STK3 overexpression reverses the CHRDL2 -induced growth and proliferation abilities and cell cycle transition of GC cells. Representative figures are shown. Data is shown as the mean ± SD. All results were obtained from three independent experiments. *$p < 0.05$; **$p < 0.01$; ***$p < 0.001$.

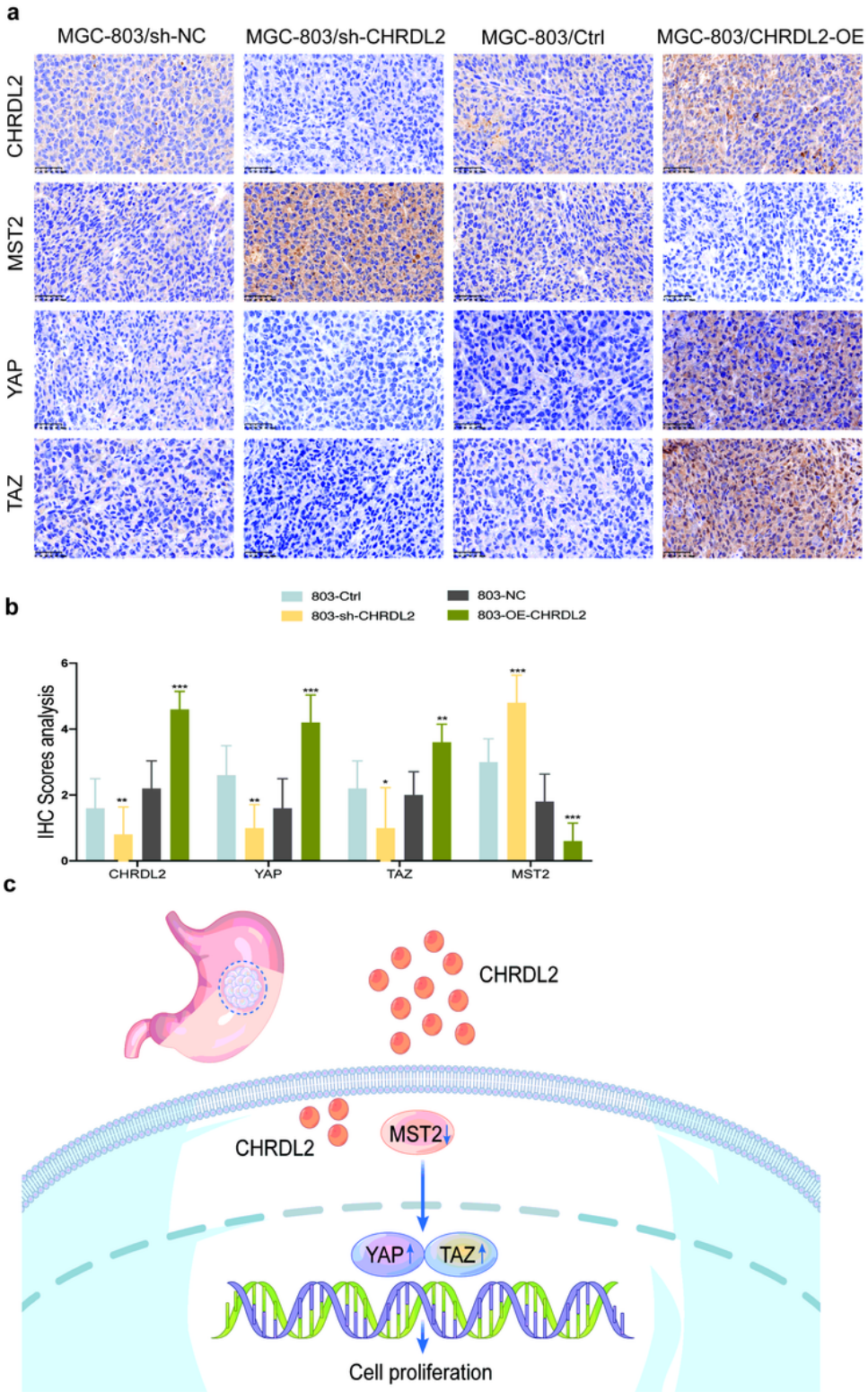

Figure 6

The correlation between CHRDL2, YAP, TAZ, and MST2 in subcutaneous tumors. a In the CHRDL2 silencing group, the expression of YAP and TAZ were reduced and MST2 was upregulated as determined by IHC staining analysis, while the opposite results were shown in the CHRDL2 overexpressing group. Representative figures are shown. Scale bar: 50 μm. **b** Proposed model depicting that CHRDL2 can regulate cell proliferation and influence the cell cycle by activating the YAP/TAZ signaling pathway in GC cells.

Supplementary Files

This is a list of supplementary files associated with this preprint. Click to download.

- suptables1s2.docx